Effect of activation method on Fe FTS catalysts: investigation at the site level using SSITKA

Kandis Sudsakorn,[a] James G. Goodwin, Jr.,[b,*] and Adeyinka A. Adeyiga [c]

[a] *Department of Chemical and Petroleum Engineering, University of Pittsburgh, Pittsburgh, PA 15261, USA*
[b] *Department of Chemical Engineering, Clemson University, Clemson, SC 29634, USA*
[c] *Department of Chemical Engineering, Hampton University, Hampton, VA 23668, USA*

Abstract

Proper activation of Fe catalysts is an important step in determining their activity for the Fischer–Tropsch synthesis (FTS). The results of this study reveal for the first time the effect of activation and time on stream (TOS) on intrinsic site activity and concentration of surface intermediates during CO hydrogenation (methanation) on an Fe FTS catalyst. The catalyst was activated under identical conditions but with different pretreatment gases: CO ([CO]), H_2 ([H]), or syngas ([S]). Lifetime (τ_M) and concentration of methane surface intermediates (N_M) were measured in situ using isotopic tracing (SSITKA) of CO hydrogenation under methanation conditions ($H_2 : CO = 10 : 1$, $T = 280\,°C$, $P = 1.8$ atm). Fe phases after activation were found by XRD to be $Fe^0 + Fe_3O_4$ for [H] and Fe carbides + Fe_3O_4 for both [CO] and [S]. Reaction and SSITKA results showed that the rate and abundance of surface intermediates on the [H]-pretreated catalyst developed with TOS, reaching a maximum at ca. 1 h, and then declined to steady-state values at 21 h, still significantly higher than for the other pretreated samples. Activity was shown by SSITKA to be primarily determined by the number of active intermediates (related to the number of surface sites). Measures ($1/\tau_M$) of the intrinsic site activity on the differently activated catalyst samples were not significantly different, suggesting that the active sites were all identical. Given the similarity in the activity of the sites and the increase in the concentration of active sites (and rate) of [H] and [CO] during the initial reaction period, it can be concluded that the active sites are probably on a (partially?) carburized Fe surface.
© 2002 Elsevier Science (USA). All rights reserved.

Keywords: Activation of Fe; Fe FTS catalysts; Spray-dried Fe catalysts; SSITKA; Isotopic tracing; Pretreatment effects; Active sites; Site activity; Fischer–Tropsch synthesis

1. Introduction

Extensive phase changes of Fe Fischer–Tropsch (FT) catalysts during activations and especially during FTS make Fe the most complicated system among FT catalysts (including Ni, Co, and Ru). The catalytically active phase of the other metals is well known to be the metal state. Several phases of iron have been found to coexist during the FT reaction [1–4], including metallic Fe (α-Fe), Fe oxides, and Fe carbides [5]. The proportion of these Fe phases can be varied, depending upon reaction conditions and activation procedures, which determine the initial state of the catalyst before reaction. The catalytically active phase(s) in a working Fe catalyst for FTS has been debated extensively by researchers. The active

Fe phases have been concluded by different researchers to be mainly Fe oxides (especially Fe_3O_4) [6–10], Fe carbides [11–14], or Fe metal [4]. However, other possible active Fe phases have also been suggested, such as a surface phase on Fe_3O_4 [15].

Due to the above complexity, investigation into the active forms of Fe in a working catalyst requires an in situ technique with sufficient spatial resolution. Unfortunately, most of the techniques used to study iron catalysts in the past, including Mössbauer spectroscopy, XRD, and XPS, are not capable of providing such resolution [5]. The conclusion has been reached by some [16–18] that the exact relationship between Fe phase composition and reactivity of the catalyst may not be able to be made.

The focus of the research reported here was on characterizing the kinetic nature of the active sites of an Fe catalyst pretreated in different ways. The effects of different activa-

---

tions (H_2, CO, or syngas) were investigated. It was also desired to determine how the active sites generated changed with reaction time on stream (TOS). Steady state isotopic-transient kinetic analysis (SSITKA), first developed by Happel [19], Bennett [20], and Biloen [21], is a powerful technique capable of assessing the surface kinetics of catalytic reactions in situ. Previously, this isotopic tracing technique had been successfully used to study the product chain growth during CO hydrogenation on Fe [22,23] and the carbon pathways on Fe/Al_2O_3 [24]. However, neither of these studies investigated the effect of pretreatment on Fe activity. The results of this study permit us to better understand activity development at the site level of an Fe catalyst after activation and during FTS. By using this isotopic tracing technique, the intrinsic site activities and concentrations of surface intermediates developing with TOS during Fe FTS are revealed for the first time.

2. Experiment

2.1. Catalyst

The Fe catalyst used for this study was prepared by precipitation and then spray drying. The relative compositions by weight percentage were $100Fe/5Cu/4.2K/11SiO_2$. The details of catalyst preparation have been given elsewhere [25–27]. Briefly, a mixture containing the desired ratios of Fe, Cu, and Si was precipitated at room temperature with ammonium hydroxide solution. The resulting precipitate was filtered, washed, and then mixed with the desired ratio of $KHCO_3$ solution. The reslurried precipitate was then spray dried at 250 °C in a Niro spray drier and calcined at 300 °C for 5 h in a muffle furnace. The calcined catalyst was sieved to particle sizes between 38 and 90 µm before use.

2.2. Catalyst activation

All the gases used for this study were ultra-high-purity grade. A 0.1-g catalyst sample was loaded into the reactor and pretreated with either H_2, CO, or syngas ($H_2:CO = 2:3$). Each pretreatment was carried out under identical conditions at 280 °C for 12 h with a ramp rate of 1 °C/min from room temperature, a gas flow rate of 5 ml/min, and a total pressure of 1 atm.

2.3. Catalyst nomenclature

The following nomenclatures are used to refer to the three different pretreatments and pretreated catalyst samples: [H] for H_2-, [CO] for CO-, and [S] for syngas-pretreated samples. The original calcined catalyst is referred to as P9 to indicate that it contains 9 wt% precipitated (P) SiO_2.

2.4. Catalyst characterization

A Scintag 2000 X-ray diffractometer with monochromatized Cu-K_α radiation (40 kV, 40 mA) and a Ge detector were used to determine powder XRD patterns of the activated and passivated catalyst samples. Each sample was analyzed, using a step scan mode at a scan rate of 0.02° (2θ) per second from 10° to 80°. XRD peak identification was done by comparison to the JCPDS database software.

BET surface areas, pore volumes, and average pore sizes of the activated and passivated catalyst samples were measured by N_2 physisorption using a Micromeritics ASAP 2010 automated system. Each catalyst sample was degassed under vacuum at 100 °C for 1 h and then 300 °C for 2 h prior to each measurement.

Both H_2 and CO chemisorption were done on the [H]- and [CO]-activated Fe catalyst samples with a Micromeritics Chemisorption ASAP 2010 automated system. H_2 chemisorption was performed at 35 °C following the procedure used in Ref. [28] assuming the ratio H chemisorbed : Fe^0 surface atom = 1 : 1. Prior to H_2 chemisorption, the catalysts were evacuated to 10^{-6} mm Hg at 100 °C for 60 min, pretreated in flowing (50 ml/min) H_2 for [H] or CO for [CO] at 100 °C for 5 min, pretreated in flowing H_2 or CO at 280 °C for 12 h after ramping up at a rate of 1 °C/min, and then evacuated at 10^{-6} mm Hg and 280 °C for 90 min to desorb any hydrogen or CO. For CO chemisorption, the catalyst sample was treated under the same condition as described above prior to the measurement but the analysis was carried out at 25 °C. It should be noted that CO chemisorption on Fe by Emmett and Brunauer [29] was done at -183 °C, assuming an average CO : Fe_s^0 stoichiometry of 1 : 2. However, due to the limitation of the Micromeritics system, chemisorption at that low a temperature was not possible; thus, the CO chemisorption reported in this study was done at 25 °C.

2.5. SSITKA reaction system

A schematic diagram and the detailed configuration of the SSITKA reaction system used in this study have been given elsewhere [30]. In brief, a quartz microreactor with ID of 4 mm was used with a thermocouple installed on top of the catalyst bed for temperature readings. A pneumatic valve operated electrically was used to switch between two feed streams into the reactor having the same flow rates but containing different isotopic labeling of the reactant species (^{12}CO vs ^{13}CO). The flow rate and pressure of the two feed streams were maintained constant during the switching using two backpressure regulators installed on the reactor effluent line and a vent line. The gas lines used in the system were designed to be as short as possible to minimize gas phase holdup in the system. The gas lines exiting from the reactor were maintained at 220 °C to prevent blockage by heavy hydrocarbon deposits. The effluent gas was analyzed by an online gas chromatograph (Varian CP-3800) and a

Table 1
Catalyst properties after activation and passivation

Pretreatment	Fe phases[a] (after pretreatment)	N_2 physisorption[b]		
		BET s.a. (m^2/g)	Pore volume (cm^3/g)	Average pore size (Å)
Original calcined	Fe_2O_3	148	0.15	40
[H]	$Fe^0 + Fe_3O_4$	56	0.19	129
[S]	Fe carbides $+ Fe_3O_4$	58	0.14	98
[CO]	Fe carbides $+ Fe_3O_4$	76	0.13	68

[a] Determined by XRD.
[b] Error $= \pm 5\%$ of the value measured.

quadruple mass spectrometer (Pfeiffer Vacuum) equipped with a high-speed data-acquisition system interfaced to a personal computer using Balzers Quadstar 422 v 6.0 software (Balzers Instruments).

2.6. Kinetic measurements

After pretreatment the catalyst bed was purged with 30 ml/min of He for 15 min while the temperature was maintained at 280 °C. At this temperature, the reaction mixture containing 2 ml/min of CO, 20 ml/min of H_2, and 80 ml/min of He was then introduced into the reactor. The system was pressurized to 1.8 atm and maintained at this pressure. Step changes were made between ^{12}CO and ^{13}CO as the reaction proceeded with TOS, without disturbing the other reaction conditions. It should be noted that ^{12}CO contained 5 vol% of Ar in order to determine the gas phase holdup in the reaction system. The details for calculation of SSITKA parameters (the average surface lifetime (τ) and the concentration of active surface intermediates (N)) are given elsewhere [35].

3. Results and discussion

3.1. Catalyst properties

Table 1 shows the N_2 physisorption properties and the major phases of Fe after different pretreatments. XRD patterns of all the catalyst samples studied are shown in Fig. 1, with the most intense diffraction peaks for each Fe phase evident indicated. As expected, the fresh calcined catalyst as prepared was in the form of hematite, Fe_2O_3. The major Fe phases of [H] were found to be Fe metal and magnetite, Fe_3O_4, while those of [CO] and [S] were mostly Fe carbides with only a small trace of Fe_3O_4 (its most intense peak being at 2θ of ca. 35.5 °). The presence of this small amount of Fe_3O_4 after [CO]-activation was even clearer in a previous study for a different composition of spray-dried Fe catalyst [31]. Identification of exact carbide forms is usually difficult due to the overlapping of their diffraction peaks [32]. For example, an intense peak between 2θ of 43° and 44° has been reported to be characteristic of both ε'-$Fe_{2.2}C$ and χ-Fe_5C_2 [33]. Both carbide phases have been found after similar pretreatments (although not

identical conditions) by other researchers using XRD and Mössbauer spectroscopy [32,34]. Therefore, it is concluded that for this study [CO] and [S] also contained a mixture of these two carbides as majority phases after pretreatment.

BET surface area (Table 1) of the catalyst was found to decrease by more than 50% for all pretreatments, while the porosity remained almost unchanged. The average pore size of the catalyst was found to be significantly larger in all pretreated samples. These changes in N_2 physisorption properties after pretreatment for precipitated Fe catalysts are commonly known to result from sintering of the iron pore structure. The results for P9 are in good agreement with our results for other precipitated Fe catalysts reported previously [31].

Both H_2- and CO-chemisorption data of [H] and [CO] are summarized in Table 2. These measurements for [S] were not carried out since the chemisorption system was not set up to pretreat with syngas. As shown in Table 2, [H] had higher values of total gas chemisorbed for both H_2 and CO. It should be noted that the total amount of H_2 chemisorbed for [H] was higher than the total CO chemisorbed. However, [CO] was found to exhibit the opposite, with more CO being adsorbed than H_2.

3.2. Catalyst performance during methanation

Both total rate (rate of CO converted) and rate of methane formation vs TOS of the differently pretreated samples are
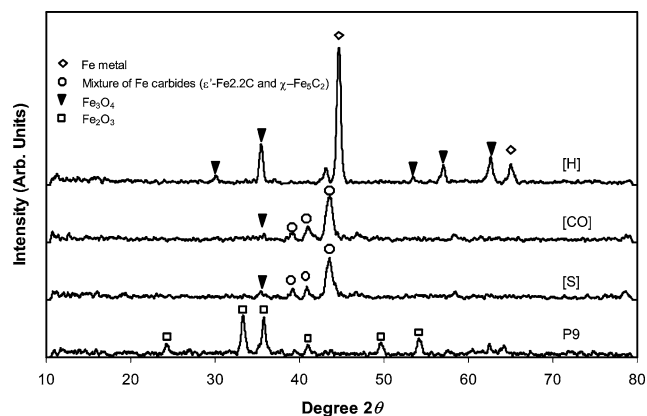

Fig. 1. XRD patterns of the original calcined and differently activated catalyst samples.

Table 2
Chemisorption on the activated P9 catalyst

Pretreated catalyst samples	CO chemisorption[a]		H₂ chemisorption[a]	
	Total (μmol CO/g-cat)	Metal dispersion[b] (%)	Total (μmol H₂/g-cat)	Metal dispersion[b] (%)
[H]	26.7	2.6	41.2	4.0
[CO]	8.0	0.8	4.5	0.4

[a] Error $= \pm 5\%$ of values measured.
[b] Based on total Fe content in the catalyst as prepared, assuming $H/Fe_s^0 = 1$ and $CO/Fe_s^0 = 0.5$.

presented in Fig. 2. Although the same catalyst was used, the resulting rates (total and methane formation rates) after the different pretreatments were found to be significantly different, indicating that the pretreatments had a significant influence on the Fe catalyst that affected directly catalyst performance during reaction. The methane selectivity vs TOS of each of the differently pretreated samples is shown in Fig. 3. The initial rates of reaction on the [H] and [CO] activated samples (not shown in Fig. 2) were so low as to be difficult to accurately measure. The [S] activated sample exhibited an initial rate close to its steady-state rate, as would be expected due to the nature of its pretreatment. The activity of [H] increased rapidly and reached a maximum of ca. 1.4 μmol/g-cat/s within the first hour of the reaction and then decreased more slowly due to deactivation to steady-state operation after 13 h TOS. The activity of [H] under these reaction conditions remained higher than that of [CO] and [S] even at steady state. [CO] also showed an initial increase in rate, but an order of magnitude less than [H].

Comparing the results of the different pretreatments, the rates of [CO] and [S] were found to be very similar at steady state. Throughout the whole course of reaction after the initial first hour, [H] exhibited a significantly higher rate of CO conversion and methane formation than [CO] or [S] (Fig. 2) although its methane selectivity was found to be significantly lower (Fig. 3). Usually, H₂-pretreatment results in less active catalysts for FTS than CO and syngas. Here, [H] was probably more active than [CO] and [S] due to the
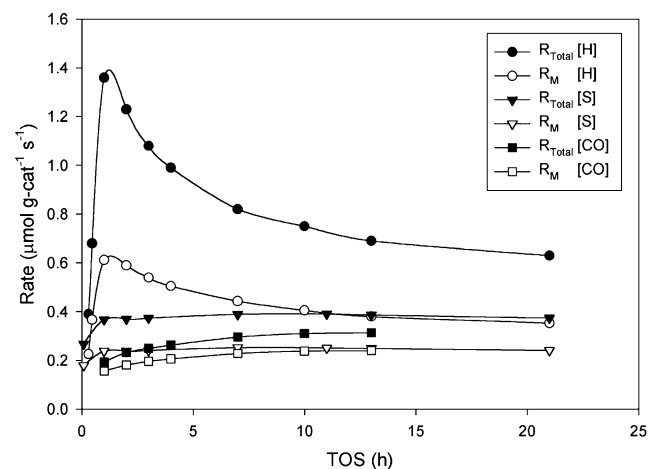
fact that methanation conditions (H₂/CO = 10) were used. Under more typical FTS conditions (low H₂/CO ratios), H₂-pretreated catalysts would be more susceptible to rapid deactivation due to carbon deposition that would mask its potential for high activity.

Obviously, the [S] pretreated catalyst was able to produce a slate of products during syngas pretreatment at a H₂/CO ratio of 2/3. However, as can be seen from the various figures, these products, some of which were undoubtedly on the surface at the start of methanation, did not seem to impact in any significant way the methanation reaction that followed. The catalyst was extremely stable once the methanation reaction was started at a H₂/CO ratio of 10/1, and the catalyst exhibited reaction stability. Only in the first hour was there any significant change and then only about a 30% increase in activity (expected due to the higher relative concentration of H₂).

3.3. Surface reaction parameters

Steady state isotopic transient analysis (SSITKA) allows one to measure in situ under actual reaction conditions the intrinsic surface residence time (τ) and the concentration of the most active surface reaction intermediates (N). Typical isotopic transients collected by mass spectrometry after isotopic switching for this Fe catalyst are shown in Fig. 4. Surface residence time of active intermediates of a species was calculated based on the difference between the peak area of that species and the peak area of Ar, since Ar was not involved in the reaction and can be used to determine the

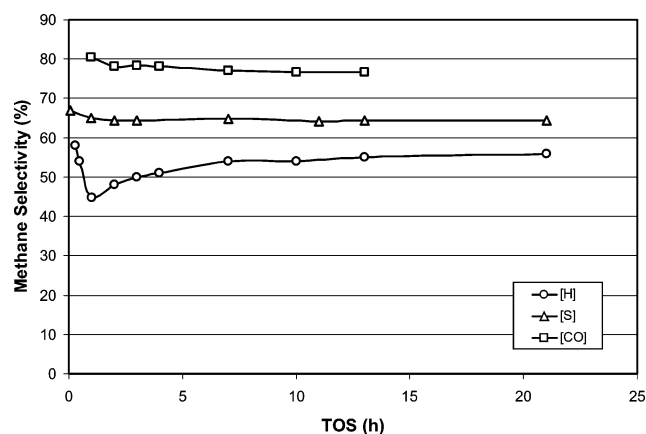Fig. 2. Total rate and rate of methane formation vs TOS on the differently activated samples.

Fig. 3. Methane selectivity vs TOS on the differently activated samples.
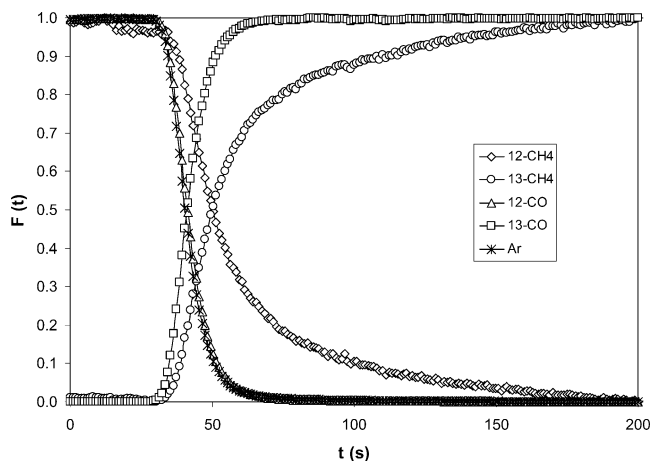
Fig. 4. Typical normalized transients for the [H]-activated Fe catalyst during CO hydrogenation.

average gas phase holdup in the entire reaction system. The concentration of active surface methane intermediates, N_M, was determined by

$$N_M = \tau_M R_M,$$

where τ_M is the surface residence time for methane formation and R_M is the rate of methane formation. Details about SSITKA and the calculation of parameters can be found elsewhere [35].

Figure 5 shows the reproducibility in measurements of methanation rate and surface lifetime (τ_M) of active intermediates to form methane for selected runs with H_2 pretreated samples. The data were highly reproducible, with the largest error in τ_M of ca. ± 0.3 s. Other runs (not shown here) were found to have the same degree of reproducibility. Figure 6 shows a comparison of the pseudo-first-order intrinsic activity (k_M), which is the inverse of the average surface residence time of the surface intermediates leading to methane (τ_M), with TOS for the differently pretreated samples. A comparison of the surface concentrations of methane intermediates (N_M) with TOS is presented in Fig. 7.
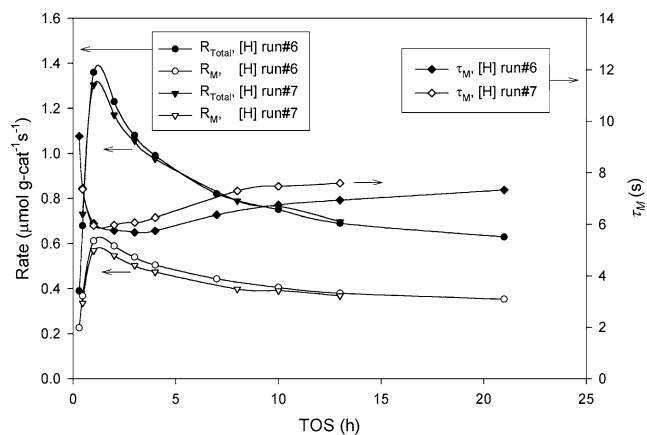

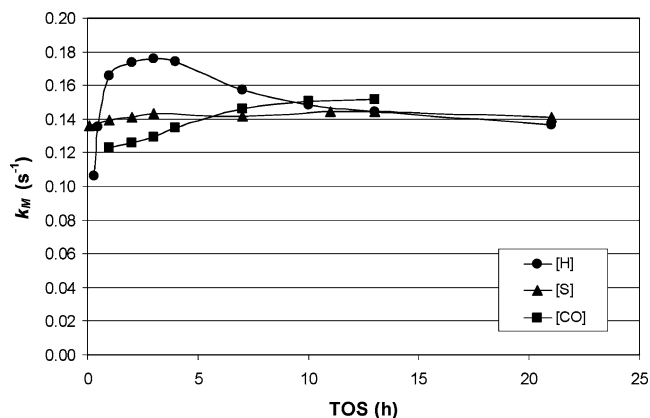Fig. 5. The reproducibility of rate and τ measurements for [H]-activated samples.

Fig. 6. Effect of activation on the development of intrinsic site activity with TOS.

If one compares the reaction results to the results for BET (Table 1) one sees that the BET results do not predict catalyst activity in any meaningful way. This is to be expected since reaction is more affected by the phase(s) of Fe present than by the total surface area.

It is interesting to compare the results for CO and H_2 chemisorption (Table 2) to those for N_M. It can easily be seen that the number of methane intermediates is only a small fraction of the amount of H_2 or CO adsorbed. SSITKA of methanation on Fe, Co, Pt, and Ru always determines that the number of active intermediates (related to the number of sites) is less than 10–15% of the number of metal surface atoms as determined by chemisorption. This can be explained in part by the fact that during the reaction the rest of the surface atoms are mainly covered by CO, which desorbs without reacting. What is not known is to what degree these other surface atoms can also become active sites for methanation. However, it is clear that neither H_2 nor CO chemisorption predicts well the behavior of the [H]- or [CO]-pretreated catalysts. It has been found over many years and for many studies that N_M measured by SSITKA provides a more direct indication than chemisorption as to why some catalysts are more active than others.
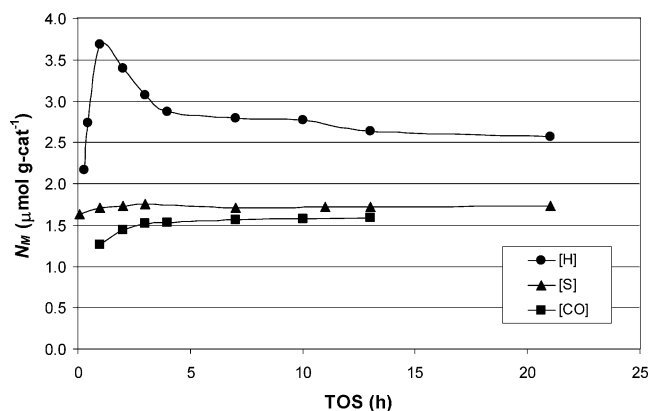

Fig. 7. Effect of activation on the development of concentration of methane intermediates with TOS.

It is clear from Figs. 2, 6, and 7 that the higher activity of the [H]-pretreated catalyst was due to having a higher concentration of active intermediates—related to having undoubtedly more active sites. τ_M measured is the residence time of carbon leading to the formation of methane averaged over all the sites. Consequently, the pseudo-first-order rate constant, $k_M = 1/\tau_M$, is also an average value. Since k_M is equal to rate/N_M, where N_M is the concentration of active methane intermediates, it is a form of TOF, having units of $1/s$. Even though any hydrogen dependency appears in k_M rather than N_M, given the constant reaction conditions for the differently pretreated catalyst samples studied, the value of k_M can be considered to be a measure of the average value of site activity. While this measure of the site activity (k_M) did become slightly higher for [H] than for [CO] or [S], the difference was relatively small. The fact that these k_M values are so similar can be considered to indicate that intermediate/site activities on all the variously pretreated catalyst samples were essentially identical. This suggests that the active sites on all the differently pretreated samples were also essentially identical and leads one to conclude that the active site of an Fe catalyst for FTS is unique—be it metal, carbide, or oxide.

As seen from Fig. 7, N_M of [H] increased rapidly within the first hour TOS as the catalyst started to be carburized once exposed to reactants. Figure 2 shows that the activity decreased rapidly during 1–4 h TOS and then continued to decline slowly to reach steady state ca. 20 h TOS. This deactivation was caused by a significant loss in concentration of methane surface intermediates (Fig. 7), while the nature of active sites did not change significantly within that period (Fig. 6). Although [CO] showed a small increase in k_M with TOS (Fig. 6), it was essentially constant. N_M of [CO] obviously increased during the initial reaction period (TOS < 1 h) and was the cause of the increase in rate for that catalyst sample as well. Both k_M and N_M of [S] were found to be essentially constant over 21 h TOS and exhibited values similar to those of [CO] after 1 h TOS throughout the whole course of reaction, taking into account the error of the measurements.

Considering all these results, it can be suggested that the active FT site is probably located on a (partially?) carburized Fe surface. Activities of [CO]- or [S]-pretreated Fe surfaces are lower than that of a [H]-pretreated one due to having fewer active sites available. This is probably due to blockage of potential active sites by carbon during pretreatment with CO or syngas having a high concentration of CO. However, it is also possible that less carburization is more optimal in generating the largest concentration of active sites.

4. Conclusion

This study explored for the first time the effect of activation and TOS on site activity and concentration of surface reaction intermediates on an Fe FT catalyst, as determined by SSITKA. It was found that activity was primarily determined by the number of active intermediates, which were quite different for differently pretreated samples during the initial stage of the reaction. However, at steady state, the concentration of methane surface intermediates on [CO] and [S] were quite similar while that for [H] remained significantly higher. [H] probably remained more active at steady state due to the use of methanation reaction conditions, which resulted in less deactivation. It was, thus, never exposed to such high partial pressures of CO as [CO] or [S]. Taking into account the error of measurement, [H], [CO], and [S] exhibited essentially identical intrinsic site activity, suggesting that the active sites on these differently activated Fe samples were all identical. The results support an earlier conclusion that the active sites for CO hydrogenation on Fe catalysts are probably on a (partially?) carburized Fe surface [11–13].

References

[1] H. Jung, W.J. Thomson, J. Catal. 134 (1992) 654.
[2] H. Jung, W.J. Thomson, J. Catal. 139 (1993) 375.
[3] G. LeCaer, J.M. Dubois, M. Pijolat, V. Perrichon, P. Bussiere, J. Phys. Chem. 86 (1982) 4799.
[4] J.W. Niemantsverdriet, A.M. van der Kraan, W.L. van Dijk, H.S. van der Baan, J. Phys. Chem. 84 (1980) 3363.
[5] M.D. Shroff, D.S. Kalakkad, K.E. Coulter, S.D. Köhler, M.S. Harrington, N.B. Jackson, A.G. Sault, A.K. Datye, J. Catal. 156 (1995) 185.
[6] F. Blanchard, J.P. Reymond, B. Pommier, S.J. Teichner, J. Mol. Catal. 17 (1982) 171.
[7] J.P. Reymond, P. Meriaudeau, S.J. Teichner, J. Catal. 75 (1982) 39.
[8] C.S. Kuivila, P.C. Stair, J.B. Butt, J. Catal. 118 (1989) 299.
[9] J.B. Butt, Catal. Lett. 7 (1991) 61.
[10] J.B. Butt, Catal. Lett. 7 (1991) 83.
[11] J.A. Amelse, J.B. Butt, L.J. Schwartz, J. Phys. Chem. 82 (1979) 58.
[12] R.A. Dictor, A.T. Bell, J. Catal. 97 (1986) 121.
[13] G.B. Raupp, W.N. Delgass, J. Catal. 58 (1979) 348.
[14] G.B. Raupp, W.N. Delgass, J. Catal. 58 (1979) 361.
[15] C.-S. Huang, L. Xu, B.H. Davis, Fuel Sci. Technol. Int. 11 (1993) 639.
[16] R.B. Anderson, The Fischer–Tropsch Synthesis, Academic Press, Orlando, FL, 1984.
[17] M.E. Dry, in: J.R. Anderson, M. Boudart (Eds.), Catalysis—Science and Technology, Vol. 1, Springer, New York, 1981, p. 159.
[18] R.J. O'Brien, L. Xu, D.R. Milburn, Y.-X. Li, K.J. Klabunde, B.H. Davis, Top. Catal. 2 (1995) 1.
[19] J. Happel, Chem. Eng. Sci. 33 (1978) 1567.
[20] C.O. Bennett, in: A.T. Bell, L.L. Hegedus (Eds.), Catalysis Under Transient Conditions, in: ACS Symposium Series, Vol. 178, Am. Chem. Society, Washington, DC, 1982, p. 1.
[21] P. Biloen, J. Mol. Catal. 21 (1983) 17.
[22] C.A. Mims, L.E. McCandlish, J. Am. Chem. Soc. 107 (1985) 696.
[23] C.A. Mims, L.E. McCandlish, J. Phys. Chem. 91 (1987) 292.

[24] D.M. Stockwell, D. Bianchi, C.O. Bennett, J. Catal. 113 (1988) 13.

[25] K. Jothimurugesan, J.G. Goodwin Jr., S.K. Santosh, J.J. Spivey, Catal. Today 58 (2000) 335.

[26] K. Jothimurugesan, J.G. Goodwin Jr., J.J. Spivey, S.K. Gangwal, in: Symposium on Syngas Conversion to Fuels and Chemicals, Proceedings of 217th National Meeting of the American Chemical Society, Anaheim, CA, March 21–25, 1999.

[27] K. Jothimurugesan, J.J. Spivey, S.K. Gangwal, J.G. Goodwin Jr., in: A. Parmaliana, et al. (Eds.), Natural Gas Conversion V, in: Studies in Surface Science and Catalysis, Vol. 119, Elsevier Science, New York, 1998, p. 215.

[28] J.S. Hwang, K.-W. Jun, K.-W. Lee, Appl. Catal. A 208 (2001) 217.

[29] P.H. Emmett, S. Brunauer, J. Am. Chem. Soc. 59 (1937) 1553.

[30] B. Chen, J.G. Goodwin Jr., J. Catal. 154 (1995) 1.

[31] K. Sudsakorn, J.G. Goodwin Jr., A.A. Adeyiga, submitted for publication, 2002.

[32] D.S. Kalakkad, M.D. Shroff, S. Kohler, N. Jackson, A.K. Datye, Appl. Catal. A 133 (1995) 335.

[33] D.B. Bukur, X. Lang, Y. Ding, Appl. Catal. A 186 (1999) 255.

[34] D.B. Bukur, K. Okabe, M.P. Rosynek, C. Li, D. Wang, K.R.P.M. Rao, G.P. Huffman, J. Catal. 155 (1995) 353.

[35] S.L. Shannon, J.G. Goodwin Jr., Chem. Rev. 95 (1995) 677.